Article

Time-Scale- and Temperature-Dependent Mechanical Properties of Viscoelastic Poly(3,4-ethylenedioxythiophene) Films

A. Robert Hillman, Igor Efimov, and Karl S. Ryder

J. Am. Chem. Soc., **2005**, 127 (47), 16611-16620• DOI: 10.1021/ja054259z • Publication Date (Web): 05 November 2005

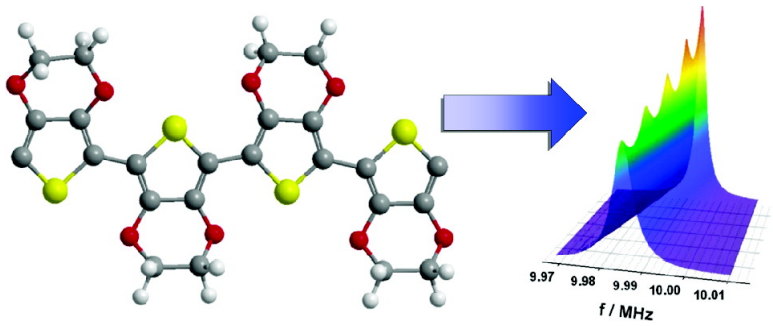

More About This Article

Additional resources and features associated with this article are available within the HTML version:

- Supporting Information
- Links to the 4 articles that cite this article, as of the time of this article download
- Access to high resolution figures
- Links to articles and content related to this article
- Copyright permission to reproduce figures and/or text from this article

View the Full Text HTML

J|A|C|S
ARTICLES
Published on Web 11/05/2005

Time-Scale- and Temperature-Dependent Mechanical Properties of Viscoelastic Poly(3,4-ethylenedioxythiophene) Films

A. Robert Hillman,* Igor Efimov, and Karl S. Ryder

Contribution from the Department of Chemistry, University of Leicester, Leicester LE1 7RH, U.K.

Received June 28, 2005; E-mail: arh7@le.ac.uk

Abstract: The viscoelastic properties of thin films of poly(3,4-ethylenedioxythiophene) (PEDOT) have been studied using the method of acoustic impedance. The films were deposited on the Au electrodes of 10 MHz AT-cut quartz thickness shear mode resonators and exposed to acetonitrile solutions of 0.1 M $TEABF_4$ and $LiClO_4$. For p-doped films, admittance spectra as a function of potential (*E*), temperature (*T*), and time scale (frequency, via harmonics, in the range 10−110 MHz) were acquired. Shear modulus components extracted from these responses surprisingly showed virtually no variation with *E* (and thus film solvation) or with *T*, but the variation with frequency was dramatic. This qualitative behavior and the numerical values of the shear moduli contrast strongly with recently reported data for the related poly(3-hexylthiophene) system, which shares the same conducting spine but differs substantially in the substitution pattern. Accordingly, the models and interpretation for PEDOT are quite different: film dynamics are determined by free-volume effects, and side-chain motion is not a significant factor. Qualitatively similar potential and time-scale effects were seen for n-doped PEDOT, but the scope of the measurements was limited by film stability.

Introduction

Overview. In this paper, we explore the viscoelastic properties of thin films of poly(3,4-ethylenedioxythiophene) (PEDOT) surface immobilized on acoustic wave resonators. Although the properties of this material have attracted huge interest, both in terms of fundamental issues and technological applications, the crucial area of polymer dynamics has largely been ignored to date. By the combined use of applied potential, temperature, and time scale, we are able to explore the polymer dynamics in unprecedented detail. Despite the obvious strong similarities, from an electrochemical perspective, to poly(alkylthiophenes), we find that PEDOT polymer dynamics are dominated by factors different from those that govern *regioregular* poly(3-hexylthiophene). We are able to rationalize this surprising result through the novel application of models conventionally used to describe macroscopic polymer properties.

The Chemical Issue. Much of the (vast) early literature on electrodeposited conducting polymer films involves unfunctionalized pyrrole, thiophene, and aniline monomeric systems.[1,2] With the principles of electronic conductivity established, interest is now focused on substituted variants of these parent systems, either as a means of tuning polymer properties (for example, electronic band structure and thereby electronic and optical properties[3−5]) or to "wire" chemically active functionalities (such as catalytic,[6] complexing,[7] or redox[1,7,8] moieties) whose electronic communication with the underlying electrode would otherwise be impractically slow. For pyrrole- and thiophene-based systems, the location on the monomer and the spatial disposition about the polymer spine of substituents have proved to be critical. When the substituent is at the 3- or 4-position, the only choices for thiophene-based systems, the more subtle feature of regioregularity arises. Regioregular and regiorandom polymers derived from 3-substituted thiophene monomers have very different electrochemical,[9] spectroscopic,[10] and mechanical[11] characteristics; the facility to control regioregularity is thus critical to exploitation of these materials.

Partly for this reason, poly(3,4-ethylenedioxythiophene) (PEDOT) has attracted huge interest.[12−15] Because the ether

(1) Chandrasekhar, P. *Conducting Polymers, Fundamentals and Applications. A practical Approach*; Kluwer Academic Publishers: Boston, 1999.
(2) *Handbook of Conducting Polymers*, 2nd ed.; Skotheim, T. A., Elsenbaumer, R. L., Reynolds, J. R., Eds.; Marcel Dekker: New York, 1998.
(3) Harrison, M. G.; Fichou, D.; Garnier, F.; Yassar, A. *Opt. Mater.* **1998**, *9*, 53−58.
(4) Demanze, F.; Cornil, J.; Garnier, F.; Horowitz, G.; Valat, P.; Yassar, A.; Lazzaroni, R.; Bredas, J. L. *J. Phys. Chem. B* **1997**, *101*, 4553−4558.
(5) Dkhissi, A.; Beljonne, D.; Lazzaroni, R.; Louwet, F.; Groenendaal, L.; Bredas, J. L. *Int. J. Quantum Chem.* **2003**, *91*, 517−523.
(6) Rodriguez, M.; Romero, I.; Sens, C.; Llobet, A.; Deronzier, A. *Electrochim. Acta* **2003**, *48*, 1047−1054.
(7) Deronzier, A.; Moutet, J.-C. *Coord. Chem. Rev.* **1996**, *147*, 339−371.
(8) Kong, Y. T.; Boopathi, M.; Shim, Y. B. *Biosens. Bioelectron.* **2003**, *19*, 227−232.
(9) Johansson, T.; Wendimagegn, M.; Svensson, M.; Andersson, M. R.; Inganas, O. *J. Mater. Chem.* **2003**, *13*, 1316−1323.
(10) Hoffman, S. V.; Jorgensen, M. *Synth. Met.* **2003**, *138*, 471−474.
(11) Jin, S.; Cong, S.; Xue, G.; Xiong, H.; Mansdorf, B.; Cheng, S. Z. D. *Adv. Mater.* **2002**, *14*, 1492−1496.
(12) Bund, A.; Neudeck, S. *J. Phys. Chem. B* **2004**, *108*, 17845−17850.
(13) Niu, L.; Kvarnstrom, C.; Ivaska, A. *J. Electroanal. Chem.* **2004**, *569*, 151−160.
(14) Pigani, L.; Heras, A.; Colina, A.; Seeber, R.; Lopes-Palacios, J. *Electrochem. Commun.* **2004**, *6*, 1192−1198.
(15) Blanchard, P.; Carre, B.; Bonhomme, F.; Biensan, P.; Pages, H.; Lemordant, D. *J. Electroanal. Chem.* **2004**, *569*, 203−210.

functionalities block both the 3- and 4-positions of the monomer (EDOT), (i) polymerization can only proceed at the 2- and 5-positions, resulting in a linear (non-cross-linked) molecule with highly extended conjugation,[16] and (ii) there is no opportunity for regioisomerism at the 3- and 4-positions. The ether substituents also lower the monomer and polymer oxidation potentials, placing less stringent demands on the electrolyte medium and giving greater polymer stability to redox cycling (doping and undoping). As a consequence of this accumulation of desirable attributes, PEDOT has been explored as a material for applications in electroluminescent[17] and electrochromic[18−20] displays as well as in electronic muscles and actuators[21,22] and others.[23,24]

Motivation. We recently[25] used acoustic impedance, a more sophisticated variant of the electrochemical quartz crystal microbalance (EQCM[26]), to study the viscoelastic properties of poly(3-hexylthiophene) (P3HT) thin films. Although it was not possible to proceed further than parametrization in terms of shear moduli for electrochemically polymerized (regiorandom) P3HT,[27] shear moduli for chemically polymerized (regioregular) P3HT could be interpreted in terms of models conventionally applied to bulk polymer mechanical properties.[25] Interestingly, film viscoelastic properties could not be explained using a model (Williams−Landel−Ferry, WLF) based on extended spinal motions but could be rationalized using an activation model based on local side-chain motion. The observed activation enthalpy of 9.7 kJ mol^{-1} is sufficiently close to the barrier of 12.5 kJ mol^{-1} for rotation around a C−C bond to suggest thermally activated rotation of alkyl side chains.

This prompts a very interesting general fundamental question with profound consequences for a number of applications. The electrochemical and electronic processes responsible for driving redox-state (doping level) switching are associated with the polymer spine. The key question is whether the mechanical (viscoelastic) properties are associated *either* also with the spine (where the valence and conduction electrons reside) *or* alternatively with the side chains. This is self-evidently crucial to applications exploiting film mechanical properties, such as microactuators. However, it is of far wider relevance because the spatial disposition and dynamics of the side chains invariably modulate the transport of counterions (dopant) required by electroneutrality to accompany spinal charge state changes that underlie essentially all applications of conducting polymers.

Surprisingly, despite the huge volume of literature on PEDOT films,[28] their viscoelastic properties have not been explored at a level that would allow the above issues to be addressed. The EQCM has been used, for acoustically thin films, as a gravimetric probe of redox-driven ion and solvent exchange between PEDOT films and their bathing solutions.[12,29] These conditions correspond to an effective time scale much shorter than the relaxation time of the polymer such that it appears "rigid". The present study extends the arena of study in three respects: it examines acoustically thick ("nonrigid") films, it explores the dynamics of the polymer rather than the mobile species, and it uses a combination of resonator harmonics, temperature, and potential as control parameters to explore an extended time-scale range of the polymer stress master relaxation curve.

Strategy. Our approach is to use the EQCM in dispersive mode, i.e., acquire the resonator admittance as a function of frequency ($f = \omega/2\pi$) in the vicinity of resonance; this provides the complete resonance feature rather than just its peak frequency. From this, we are able[30] to extract the film's complex shear modulus, $\mathbf{G} = G' + jG''$ (where G' is the storage modulus, G'' is the loss modulus, and $j = \sqrt{(-1)}$). Practically, in situ electrochemically controlled measurements are complicated by the fact that the acoustic impedances of the film, $Z_P = (\rho_f \mathbf{G})^{1/2}$ (ρ_f = film density), and of the bulk fluid, $Z_L = (j\eta_l\rho_l\omega)^{1/2}$ (η_l = liquid viscosity and ρ_l = liquid density), are of comparable magnitude for typical experimental conditions. Consequently, $\mathbf{G}$ has to be evaluated as a complex root of the exact eq 1: for

$$Z = j\omega\rho_s + Z_P\left(\frac{Z_L \cosh(\gamma h_f) + Z_P \sinh(\gamma h_f)}{Z_P \cosh(\gamma h_f) + Z_L \sinh(\gamma h_f)}\right) \qquad (1)$$

the experimentally measured impedance Z, in which h_f is the film thickness and $\gamma = j\omega(\rho_f/\mathbf{G})^{1/2}$ is the complex wavenumber for the shear acoustic wave. Equation 1 also contains the term $j\omega\rho_s$ to represent material entrapped within surface roughness features; as described below, the experimental procedures are designed to minimize this correction term.[30]

Time−Temperature Equivalence. Film viscoelastic properties, represented by $\mathbf{G}$, are a function of time scale. This is represented by the relative values of the experimental time scale ($1/f = 2\pi/\omega$) and of the relaxation time (τ) for the appropriate polymer relaxation process; thus, the goal is to explore $\mathbf{G}(\omega\tau)$. The recent advance[25] we now examine is to vary $\mathbf{G}$ via both ω and τ through resonator harmonics and temperature, respectively, and then place the data on a common scale through the principle of time−temperature equivalence.[31,32] Harmonics are rarely explored in viscoelastic studies;[33,34] temperature is a much underused variable in electrochemistry, generally, and in EQCM studies, specifically, yet, despite general appreciation for bulk polymers, time−temperature equivalence has to date only been applied to one electroactive film system, P3HT.[25,35] This presents an unprecedented opportunity to explore PEDOT dynamics and,

(16) Roncali, J. *Chem. Rev.* **1992**, *92*, 711−738.
(17) Hughes, J.; Bryce, M. R. *J. Mater. Chem.* **2005**, *15*, 94−107.
(18) Groenendaal, L.; Zotti, G.; Aubert, P. H.; Waybright, S. M.; Reynolds, J. R. *Adv. Mater.* **2003**, *15*, 855−879.
(19) Cutler, C. A.; Bouguettaya, M.; Kang, T. S.; Reynolds, J. R. *Macromolecules* **2005**, *38*, 3068−3074.
(20) Mortimer, R. J. *Electrochim. Acta* **1999**, *44*, 2971−2981.
(21) Smela, E. *Adv. Mater.* **2003**, *15*, 481−494.
(22) Careem, M. A.; Vidanapathirana, K. P.; Skaarup, S.; West, K. *Solid State Ionics* **2004**, *175*, 725−728.
(23) Pei, O.; Zuccarello, G.; Ahlskog, M.; Inganas, O. *Polymer* **1994**, *35*, 1347.
(24) Dietrich, M.; Heinze, J.; Haywang, G.; Jonas, F. *J. Electroanal. Chem.* **1994**, *396*, 87.
(25) Hillman, A. R.; Efimov, I.; Skompska, M. *J. Am. Chem. Soc.* **2005**, *127*, 3817−3824.
(26) Hillman, A. R. The electrochemical quartz crystal microbalance. In *Encyclopaedia of Electrochemistry*; Bard, A. J., Stratmann, M., Eds.; Wiley: New York, 2003; Vol. 3, pp 230−289.
(27) Brown, M. J.; Hillman, A. R.; Martin, S. J.; Cernosek, R. W.; Bandey, H. *J. Mater. Chem.* **2000**, *10*, 115−126.
(28) Roncali, J.; Blanchard, P.; Frere, P. *J. Mater. Chem.* **2005**, *15*, 1589−1610.
(29) Randriamahazaka, H.; Plesse, C.; Teyssie, D.; Chevrot, C. *Electrochim. Acta* **2005**, *50*, 1515−1522.
(30) Bandey, H.; Hillman, A. R.; Brown, M. J.; Martin, S. J. *Faraday Discuss. Chem. Soc.* **1997**, *107*, 105.
(31) Ferry, J. D. *Viscoelastic properties of polymers*, 2nd ed.; Wiley: New York, 1970.
(32) Aklonis, J. J.; MacKnight, W. J. *Introduction to Polymer Viscoelasticity*; Wiley: New York, 1983; Chapter 7.
(33) Wolff, O.; Seydel, E.; Johannsmann, D. *Faraday Discuss.* **1997**, *107*, 91−104.
(34) Johannsmann, D. *J. Appl. Phys.* **2001**, *89*, 6356−6364.
(35) Hillman, A. R.; Efimov, I.; Skompska, M. *Faraday Discuss. Chem. Soc.* **2002**, *121*, 423−439.

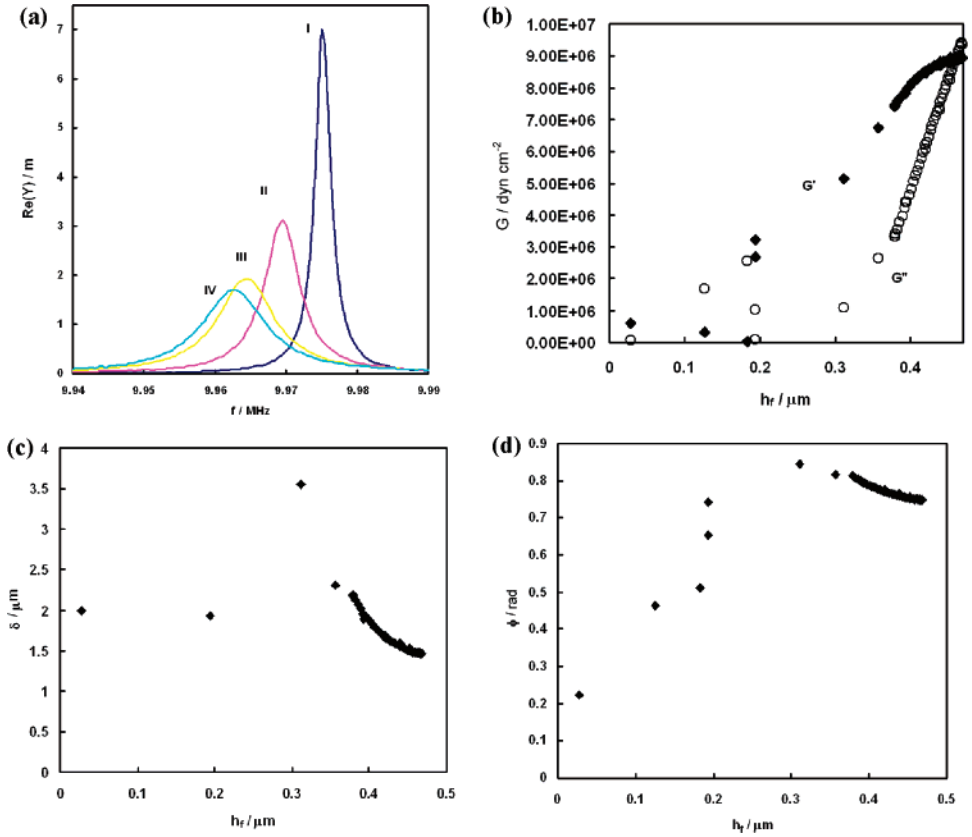

Figure 1. Real part of admittance for fundamental mode. Curves of (a) (I) bare crystal exposed to acetonitrile, (II−IV) PEDOT film at different stages of deposition. II: $h_f = 0.19$ μm, $G' = 3 \times 10^6$ dyn cm^{-2}, $G'' = 1 \times 10^6$ dyn cm^{-2}; III: $h_f = 0.31$ μm, $G' = 5 \times 10^6$ dyn cm^{-2}, $G'' = 1.1 \times 10^6$ dyn cm^{-2}. IV: $h_f = 0.47$ μm, G'=8.9 $\times 10^6$ dyn cm^{-2}, $G'' = 9 \times 10^6$ dyn cm^{-2}. Curves of (b) storage and loss moduli calculated as function of film thickness, (c) decay length (δ, as defined in text), and (d) phase shift (ϕ, as defined in text).

in particular, the issue of whether spinal or substituent motions are dominant.

In this work, the strategy and interpretational framework developed for regioregular P3HT[25] are exploited. However, the closed-ring substitution pattern of PEDOT precludes the same outcome as that for PEDOT, so the question is *what determines PEDOT viscoelastic properties*? The power of the methodology rests upon manipulating the normalized time scale $\omega\tau$ directly via harmonic frequency ($f = \omega/2\pi$), indirectly through temperature ($\tau = \tau_0 \exp(\Delta H^{\ddagger}/RT)$, and indirectly through potential (varying film solvation and thus τ_0). Through this combination, we have exceptionally wide access across the stress master relaxation curve, especially in comparison to the single-point (located in the nonviscoelastic regime) approach of conventional EQCM experiments.

Experimental Section

Materials. The solution for electropolymerization was 50 mM monomeric EDOT (Aldrich)/0.1 M tetraethylammonium tetrafluoroborate ($TEABF_4$; Aldrich) in dry acetonitrile. Reagents were used as received. The quartz resonators were 10 MHz AT-cut crystals coated with Au (ICM, Oklahoma City, OK), with piezoelectric and electrochemically active areas of 0.23 and 0.25 cm^2, respectively. Polished crystals were used to minimize the effects of surface roughness;[30,36] the small residual linear term in eq 1 was handled as described elsewhere.[37] One face of the crystal was exposed to solution to form the working electrode in a three-electrode cell with an Ag wire reference electrode and a Pt counter electrode.

Instrumentation. Crystal-impedance spectra were recorded using a Hewlett-Packard HP8751A network analyzer connected to an HP87512A transmission/reflection unit via 50 Ω coaxial cable. The electrochemical cell was immersed in a thermostatic bath, allowing measurements to be conducted over the temperature range 0−70 °C.

Procedures. PEDOT films were deposited potentiodynamically (0.0−1.25 V, 10 mV s^{-1}); the $i-E$ response was qualitatively similar to that reported in ref 14. A single cycle deposited a film with a thickness, h_f, of 0.4−0.7 μm (corresponding to a resonant frequency shift of 12−18 kHz), according to precise conditions. As will be shown below (see Figure 1), this places the system in the acoustically thick (but not semi-infinite) regime, optimum for determination of viscoelastic properties. For each film, thickness was estimated by coulometric assay using the reduction charge under a slow scan voltammetric peak for a film transferred to monomer-free 0.1 M $TEABF_4/CH_3CN$ (for the n-doping experiments; see explanation below) or $LiClO_4/CH_3CN$, using a doping level of 0.3 e per monomer unit[29] and $\rho_f = 1$ g cm^{-3}.

Data Analysis. A major part of the strategy involves determining the variation of film properties (**G**) with temperature. However, in using eq 1 to accomplish this, we must also take into account the fact that the crystal and liquid properties (and thereby Z_L) also vary with temperature. We have described elsewhere[35] the procedure for accomplishing this through "blank" experiments using bare Au/quartz crystals to determine the viscosity−density product, $\eta_l\rho_l$, for the solution as a function of temperature (T). Application of eq 1 to experimentally determined impedance data and solution using the commercial Maple software package provided the complex shear moduli, $\mathbf{G} = G' + jG''$, for the film, free of any artifacts associated with surface roughness or variations in fluid properties. The procedures for implementing and

(36) Bruckenstein, S.; Fensore, A.; Li, Z. F.; Hillman, A. R. *J. Electroanal. Chem.* **1994**, *370*, 189−195.
(37) Hillman, A. R.; Jackson, A.; Martin, S. J. *Anal. Chem.* **2001**, *73*, 540−549.

interpreting temperature-dependent "shift factors" are discussed below. Within the format of log(G) vs log(ω) plots (individually for G' and G'' components), we superimposed on the curve at the reference temperature (selected as 20 °C) the curves acquired at other temperatures by application of a lateral shift of log $a(T)$.

Results

Electropolymerization. Representative data acquired during electropolymerization and deposition of a PEDOT film are shown in Figure 1. Raw admittance spectra (real component shown in Figure 1a) at the fundamental frequency (10 MHz), commencing with the bare Au/quartz crystal immersed in solution taken at selected potentials during the anodic half of a deposition cycle, show monotonic decreases in resonant frequency and admittance as deposition proceeds. The substantial decrease in admittance (as compared to the bare resonator) indicates that we are in the acoustically thick regime, suitable for determining shear moduli. This is confirmed (see following) by the phase shift data which show that, under the conditions used, the films were not grown sufficiently thick to approach film resonance, where the response is more complicated and nonmonotonic.[38,39]

The outcome of the data fitting of G' and G'' values is shown in Figure 1b as a function of (growing) film thickness during a single deposition cycle. The nature of this process means that we are not able to explore the effects of time scale (harmonic frequency) or temperature within a single experiment, but it is clear qualitatively that the shear modulus components are consistent with a viscoelastic material. By the end of the experiment ($h_f = 0.47$ μm), the storage modulus has reached a plateau at $G' \approx 9 \times 10^6$ dyn cm^{-2}. The loss modulus has a comparable value but has not reached a plateau at this point.

We do not pursue the interpretation of the shear modulus components for the deposition process for three reasons. First, the potentiodynamic nature of this experiment means that the increase in film thickness in principle owes its origins to both a time and a potential dependence; separating the two is not possible. Second, an assumption[37] of our modeling routines is that the film is compositionally homogeneous. Although this is a reasonable approximation for a film that has been deposited, redox cycled, and relaxed at some selected potential, it is less likely to be true of a dynamically growing and evolving film. Third, this "single-shot" experiment does not permit us to use higher harmonics or temperature as control variables in the manner we describe later for films after deposition; without these probes, we have less insight.

On the basis of the G' and G'' data, we show in Figure 1c,d the decay length (a material property, defined as $\delta = [\mathrm{Re}\{j\omega/\sqrt{(\rho_f/\mathbf{G})}\}]^{-1}$, where Re indicates the real component of the quantity in braces) and the acoustic phase shift (a property of both the material and the thickness at the particular sampled point, defined as $\phi = h_f\,\mathrm{Re}\{\omega/\sqrt{(\rho_f/\mathbf{G})}\}$). The decay length is always significantly larger than the film thickness, so we never reach the semi-infinite regime. The phase shift (see Figure 1d) increases steadily until $h_f \approx 0.3$ μm and interestingly reaches a plateau even though film thickness continues to increase. This is the result of the continued change in a shear modulus (primarily in G''). Importantly, the plateau value is in the optimal range for shear modulus determination and does not approach the value of $\pi/2$ associated with film resonance and its attendant complications.

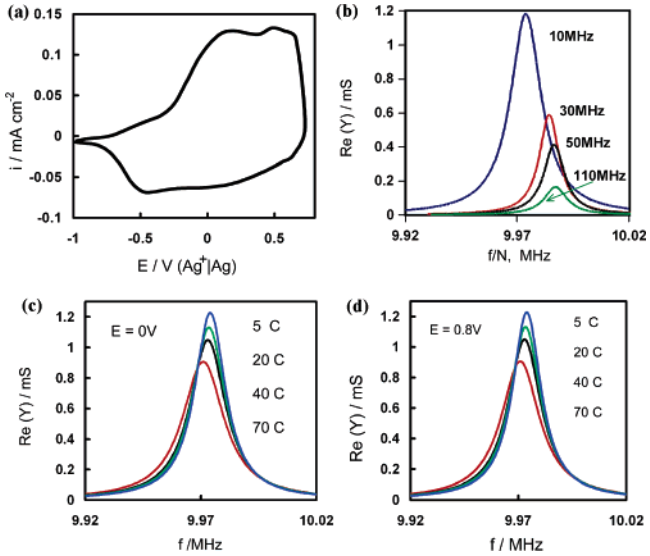

Figure 2. Composite of voltammetry and admittance spectra for E, T, and f variations for 0.45 μm thick PEDOT film in 0.1 M $LiClO_4$/acetonitrile: (a) cyclic voltammogram at $\upsilon = 20$ mV s^{-1}; (b) Re(Y) for different harmonics as a function of frequency normalized for harmonic number, N, where the characteristics of the device dictate that N assumes odd number integer values; (c) and (d) Re(Y) dispersion for the fundamental mode at various temperatures (as indicated) at (c) $E = 0.0$ V and (d) $E = 0.8$ V.

Overview of Viscoelasticity Variations. We now move to the main thrust of the study, the variation of PEDOT film shear moduli after deposition and upon exposure to background electrolyte solution. The three control variables at our disposal are resonator harmonics (effectively, frequency or time scale), temperature, and applied potential (varying small molecule, solvent and ion, content within the film). Figure 2 shows raw data that encapsulate qualitatively the key $\mathbf{G}(\omega,T,E)$ features that we shall subsequently explore quantitatively.

A. p-Doping. We first consider the p-doping regime, as indicated by the voltammetric $i-E$ response of Figure 2a; although it was possible to n-dope the polymer, slow degradation over the extended intervals required to explore frequency and temperature effects precluded investigation in the same depth as that carried out for the undoped and p-doped material. Panels b−d in Figure 2 show sets of admittance spectra in which each of the primary variables is explored in the p-doping regime, $-0.2 < E/V < 0.8$. Comparing the spectra in panels c and d that, at equivalent temperatures in each case, differ only in the applied potential, we see that the combined effects of changing polymer charge state and the associated film ion and solvent populations[30] are negligible. Given the magnitude of the potential variation and the differences in shear modulus observed for some other systems,[25,27] this is at first sight surprising. Because potential is the primary electrochemical control variable, it may also be considered slightly disappointing to have so little apparent facility to manipulate **G**, but one can envisage situations in which it would be valuable to manipulate electrical properties (via potential) independently of mechanical properties.

Looking *within* panels c and d individually, we see that changing the temperature has a measurable, though not dramatic, effect to the extent of ca. 25−30% over a range of 65 °C. (In

(38) Lagier, C. M.; Efimov, O.; Hillman, A. R. *Anal. Chem.* **2005**, *77*, 335−343.
(39) Hillman, A. R.; Brown, M. J.; Martin, S. J. *J. Am. Chem. Soc.* **1998**, *120*, 12968−12969.

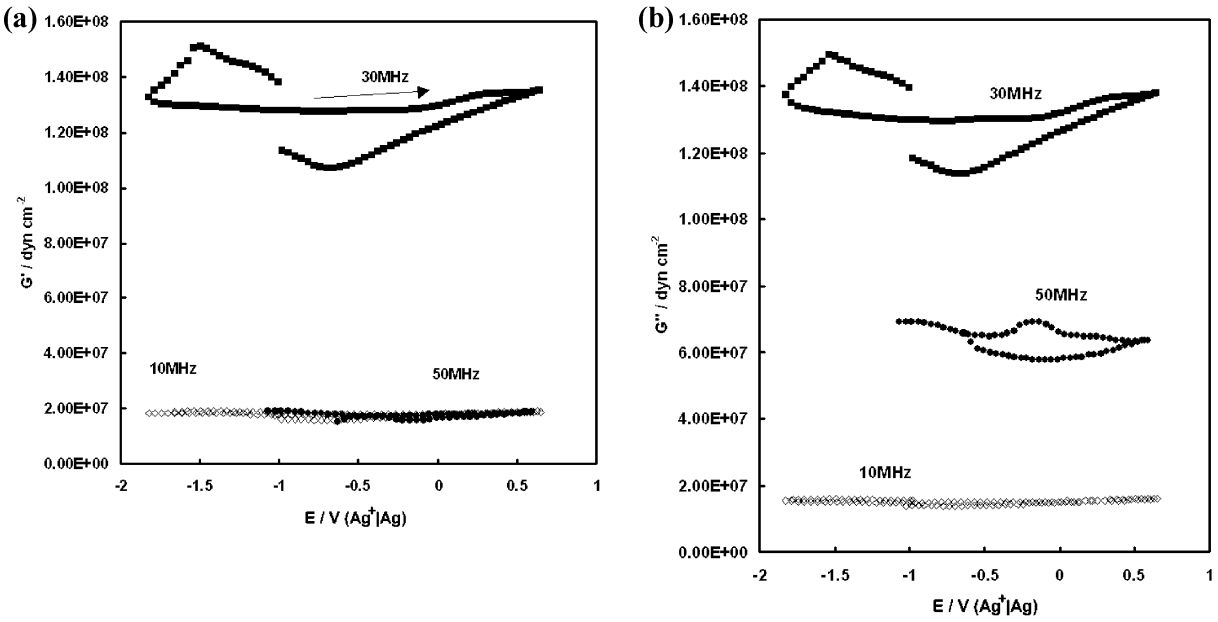

Figure 3. **G** values for broad scan n- and p-doping experiments on PEDOT in 0.1 M $TEABF_4$/acetonitrile. The scan rate is $\upsilon = 20$ mV s^{-1}. Dashed and solid lines, respectively, represent cycling in the p-doping region alone and both the n-and p-doping regions. Film thickness = 0.15 μm, $T = 20$ °C, and frequency (f) = 10, 30, and 50 MHz, as indicated.

this particular case, as indicated in the Experimental Section, simplistic appraisal of the raw data does not separate out the effect of fluid thermal variations; nonetheless, these effects are not huge and the changes associated with the polymer component discussed later are quite modest.) Inspection of panel b, in which we have placed the harmonic data (odd integer multiples of the fundamental frequency) on the same scale as the fundamental data by dividing the frequency by the harmonic number (N), shows that the observational time scale has a dramatic effect. The decreased relative frequency shift and decreased admittance with increasing observational frequency qualitatively suggest that the film becomes stiffer and lossier as the observational time scale is decreased.

To summarize, the qualitative picture of the effects of potential, temperature, and time scale, respectively, are minimal, modest, and dramatic. Our goal now is to make these observations quantitative, through shear moduli, and to rationalize them in terms of (sub)molecular contributions to polymer dynamics.

B. n-Doping. Given the relatively meager coverage in the literature of the n-doping process for PEDOT and, indeed, polythiophenes in general, we attempted to acquire viscoelastic parameters during reduction of undoped films. Preliminary experiments showed that this was not possible using a $LiClO_4$/CH_3CN medium, the electrolyte of choice for the p-doping experiments discussed later. We were therefore forced to use 0.1 M $TEABF_4$/CH_3CN for these experiments. Stability of the polymer for extended periods of time in the n-doped state unfortunately prevented acquisition of viscoelastic data on the scale described later for p-doping, but we were nonetheless able to make limited measurements, as illustrated in Figure 3. The data for both G' and G'' are qualitatively consistent with a lossy ($\tan\delta \sim 1$) material, whose properties are relatively insensitive to potential. The predominant effect seen in Figure 3 is the dependence on frequency, which is revealed in the G' and G'' values at the fundamental (10 MHz) and the third (30 MHz) and fifth (50 MHz) harmonics, acquired in that order. However, although we have shown the outcome for completeness, the data are slightly misleading in that only those at 10 and 30 MHz were reproducible. Thereafter, progressive decay (as revealed by the associated $i-E$ curves) resulted in irreproducible deterioration of the data; this problem also prevented our exploration of the effect of temperature in the n-doping regime.

Effect of Potential. Figure 4 shows shear modulus data acquired during a potentiodynamic experiment in the p-doping region for a film exposed to 0.1 M $LiClO_4$/CH_3CN. The primary goal here was an exploration of potential effects; we do not explore the effects of time scale (via harmonics) in this experiment. Looking at any *individual* data set, i.e., at *fixed* temperature (see following section for variation of temperature), there is a small amount of hysteresis in the data (as indicated by the arrows in Figure 4). We suggest that this is an effect of the film not quite managing to establish solvation equilibrium, which is generally a slower process than field-driven charge state equilibration. Given that these differences are relatively small and that there is only a small amount of hysteresis in the charge response to potential, we do not pursue this in detail. Nonetheless, strictly, this experiment differs from those described in subsequent sections, where **G** values are acquired at a fixed potential and it is reasonable to assume fully equilibrated film composition. The potentiodynamic nature of the experiment ($\upsilon = 10$ mV s^{-1}) also placed constraints upon the number of data points acquired, which limits the precision. Second, we note that although both G' and G'' increase (beyond experimental uncertainty) upon PEDOT p-doping, the effect is quite small (ca. 10%; note the highly expanded vertical scales in Figure 4).

Effect of Temperature. The voltammetric $i-E$ curves did not change significantly with temperature, with the exception of a small increase of the oxidation current near the upper anodic limit of 0.8 V. This contrasts significantly with the behavior of poly(3-hexylthiophene) films.[25] We therefore conclude that we do not need to be concerned with the two-phase behavior reported for that system.[25,27,30] This difference between the two

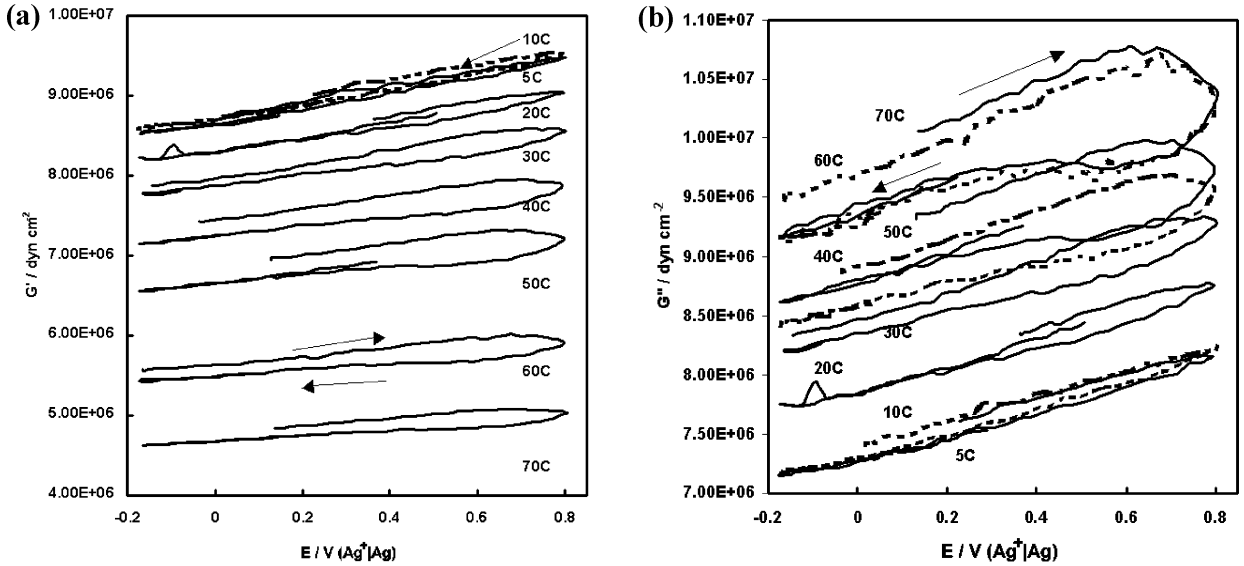

Figure 4. Shear modulus components (a) G' and (b) G'' measured at 10 MHz for p-doping of a PEDOT film in 0.1 M $LiClO_4$/acetonitrile at various temperatures, as indicated. Potentiodynamic conditions are $\upsilon = 10$ mV s^{-1}. Arrows indicate potential scan direction.

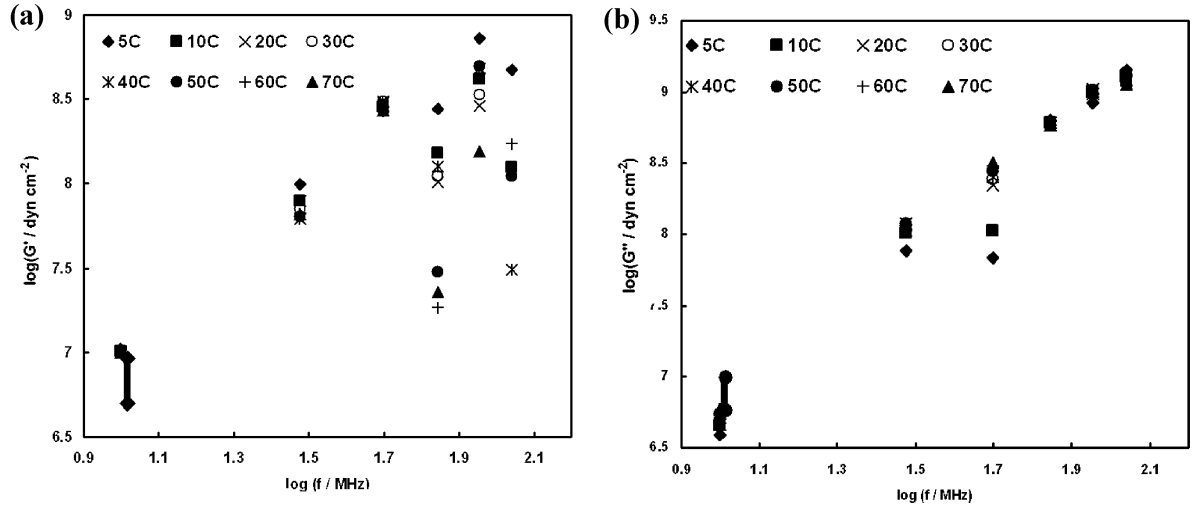

Figure 5. Double logarithmic plot of (a) G' and (b) G'' data for the PEDOT film of Figure 4, exposed to 0.1 M $LiClO_4$/acetonitrile but maintained under potentiostatic conditions ($E = 0.0$ V) as a function of acoustic wave measurement frequency (10N MHz, where the characteristics of the device dictate that N assumes odd number integer values) at various temperatures, as indicated. The vertical bars (at $f = 10$ MHz; $N = 1$) represent the spread of values seen in the potentiodynamic experiment of Figure 4 (see text).

systems, one of a number to which we draw attention, simplifies our analysis appreciably.

In addition to the potential effects described in the previous section, the data of Figure 4 for undoped and variously p-doped PEDOT also show that the effect of increasing temperature is to decrease G' (softening) and to increase G'' (greater viscous loss). Specifically, the storage modulus decreases with temperature from 9×10^6 dyn cm^{-2} at 5 °C to 5×10^6 dyn cm^{-2} at 70 °C; the effect of potential also becomes less pronounced at higher temperatures. The loss modulus increases from 7.5×10^6 dyn cm^{-2} at 5 °C to 10^7 dyn cm^{-2} at 70 °C; here, the potential dependence is unchanged with temperature.

The values of G' and G'' are of similar magnitude: their ratio, G''/G' (the loss tangent), increases from 0.83 at 5 °C, crosses through unity at ca. 30 °C, and rises to 2 at 70 °C. In the Maxwell model,[32,40] this is characteristic of a viscoelastic material whose relaxation time is approximately the same as the measurement time scale ($\omega\tau \sim 1$ in the model developed later).

Effect of Time Scale. The data in Figure 4 were acquired under potentiodynamic conditions. To focus more directly on the time-scale−temperature interaction, we also made measurements at selected fixed potentials on equilibrated (with respect to both charge state and mobile species populations) PEDOT films. The resulting G' and G'' values are presented in Figure 5a and 5b, respectively. Selected values (at the relevant potentials) of the potentiodynamic data of Figure 4, which were acquired at the 10 MHz fundamental only, are also shown in Figure 5 for comparison purposes. Given that the two data sets were acquired from different films, the agreement is rather good; with regard to the highly expanded vertical scale used for Figure 4 (in pursuit of greater scrutiny of the temperature effect), this

(40) Billmeyer, F. W., Jr. *Textbook of Polymer Science*, 3rd ed.; Wiley: New York, London, 1984.

comparison also highlights the fact that time scale (frequency) is by far the dominating factor. The variations of G' and G'' by ca. 2−2.5 orders of magnitude are substantial; they span virtually the entire viscoelastic regime and allow us to be confident about which control parameters are (or are not) significant.

The potentiostatic data of Figure 5 confirm, across an order of magnitude in the time scale, that temperature has only a minor effect on G' and G''. In the case of the G' data at higher frequency, the large scatter is partly a consequence of the fact that the signal is smaller (see Figure 2b for representative raw data). It is also the case that we have now moved into the regime where $G''/G' < 1$, and our long-standing experience is that the evaluation of the smaller shear modulus component is always associated with greater uncertainty.[25,27,30] It is clear that there is no substantial systematic variation of G' with T. The fact that the two shear modulus components are of similar magnitude indicates that $\omega\tau \sim 1$, and the fact that *both* increase with frequency suggests that the system is just below the relaxation time.[32]

Discussion

Protocols for Extraction of Shear Moduli. In developing the interpretation of the shear modulus data, it is appropriate to have an appreciation of the procedure for their extraction and of the associated uncertainties. We illustrate this through the film deposition data, starting with the raw admittance spectra. Bare Au/quartz crystals in air have a resonant resistance (at 10 MHz) of $R = 7\ \Omega$. As shown in Figure 1a, contact with acetonitrile solution results in an increase to $R = 141\ \Omega$ ($Y_{max} = R^{-1} \approx 7$ mS) and deposition of a viscoelastic PEDOT film increases this by a similar or greater amount, to a total of $R = 320\ \Omega$ ($h_f = 0.19\ \mu$m), $R = 520\ \Omega$ ($h_f = 0.31\ \mu$m), and $R = 588\ \Omega$ ($h_f = 0.47\ \mu$m). Because the contribution to the impedance by the solution is not negligible, the full eq 1 must be used for extraction of **G**.

The functional form of eq 1 is such that the calculated complex roots G' and G'' can be very sensitive to the value selected for the thickness of the film, h_f. This is particularly true at high G'.[41,42] However, there are two physical constraints on the system, a minimum value of h_f corresponding to total absence of solvent and positive values of both G' *and* G''. The former limit is straightforwardly established on the basis of coulometric data, in combination with Faraday's law and the polymer density. The second constraint is satisfied in a more sophisticated manner, as follows, in which the more extensive film characterization (cf. deposition) data allow us to exploit the additional temperature variable.

The procedure for extraction of shear moduli from acoustic admittance spectra is nontrivial because there are, in principle, four unknown parameters (film thickness, film density, and the two shear modulus components). We have previously described[37] and implemented[25] a strategy for accomplishing this in two stages, each using two measurands to provide two parameters. In the first stage, a frequency shift and coulometric data for acoustically thin films (gravimetrically interpreted) provide film thickness and density. We then assume film homogeneity so that this value of film density can be applied to acoustically thick films, and film thickness can be extrapolated from electrochemical charge data for thick films. (In the latter instance, we use redox switching rather than polymerization charge to avoid uncertainties associated with polymerization efficiency.) Thus, in the second stage of the process, one only has to fit the two shear modulus components to the admittance spectra, providing a unique solution.

We used this established procedure as a check on a newer approach that has the advantage of not relying on the extrapolation of thin film properties to thick films. We first calculated the shear modulus components as a function of systematically varied film thickness for each frequency and (in the case of film characterization) temperature measurement. In each individual set of conditions (ω, T), physically reasonable (i.e., positive) values of G' and G'' are only obtained within a relatively narrow range of h_f values. This range of possible values was slightly different for each measurement. However, regardless of the frequency (or, where varied, temperature) at which the measurement is made, the actual value of h_f is the same. Thus, correlation of these individual candidate h_f ranges defines the only value that will satisfy them all. Because each data set involves the determination of an h_f range for two shear modulus components, each at six frequencies, and (for the film characterization data) all at six temperatures, the resulting comparison of up to 72 candidate h_f ranges defines the value extremely tightly. Selected comparisons with the established methodology[25,37] showed excellent agreement, supporting the strategy and the notion that the films are in fact homogeneous.

Film Deposition Process. The data of Figure 1b allow us to explore another aspect of film (cf. material) properties that has not been explored to date, namely the variation (or otherwise) of interfacial properties with amount of surface-immobilized material. For both the G' and G'' components, the initial (short-time, low-coverage) values are low and somewhat scattered. Physically, this corresponds to a situation in which the relatively small amount of material thus far accumulated at the interface is almost certainly rather diffuse and acoustically not that different from the solution phase; this makes its characterization difficult and the output parameters somewhat uncertain. The problem is further complicated in this regime by the fact that the film may not be homogeneous, so the model used is not a good representation. After a short time (in the present case, when the thickness exceeds ca. 0.3 μm), the values of the shear modulus components adopt steady trends and the uncertainties become small. Nonetheless, in this regime, both component values steadily increase. We interpret this to imply some filling in of solvent voids by the polymer.

At some point, the amount of deposited material must be sufficient so that some length-scale independent structure is established and G' becomes independent of film thickness. This is exactly what we observe in the case of the experiment shown when $h_f > 0.45\ \mu$m. On the other hand, the loss modulus continues to change with thickness. In this particular experiment, the potentiodynamic control function means that each point corresponds to a different potential; for practical purposes, this is effectively a "different" film. The result will be a different solvation level and thereby a different extent of plasticization. This in turn alters the dissipative properties represented by G'', as observed in Figure 1b.

(41) Behling, C. The nongravimetric response of thickness shear mode resonators for sensor applications. Dip.-Phys. Dissertation, Otto-von-Guericke Universiry of Magdeburg, Germany, 1999.
(42) Lucklum, R.; Behling, C.; Hauptmann, P.; Cernosek, R. W.; Martin, S. J. *Sens. Actuators, A: Physical* **1988**, *66*, 184−192.

In appraising these G' and G'' data, it is helpful to consider the decay length and the acoustic phase shift; the former is a material property only, and the latter is a property of both the material and the sample thickness. The critical results are that the film thickness is always less than the decay length (see Figure 1c) and that the phase shift is always below $\pi/2$ (see Figure 1d). These values are consistent with the choice of model, and we do not have to be concerned about film resonance.[38,39] At low values of h_f, the small phase shift explains in part the uncertainty associated with the associated shear modulus values. We previously showed[37] that determining shear moduli for films with phase shifts less than 20° (ca. 0.4 rad) is difficult; values in excess of 30° (ca. 0.6 rad) are preferred. The plateau of the phase shift results from the fact that it is a function of both viscoelastic properties and sample thickness, which both vary and whose changing values are fortuitously compensatory.

Analysis of Shear Moduli for PEDOT Films in Background Electrolyte. We now turn to the interpretation of the G' and G'' values for PEDOT upon transfer to background electrolyte. On the basis of the recent construction of a stress master relaxation curve for a thiophene-based polymer, regioregular poly(3-hexylthiophene) (P3HT),[25] we attempted the application of the time−temperature equivalence concept (frequently expressed through the WLF equation[31]) for the PEDOT shear modulus data. For reasons we will discuss later, this was not successful. We also explored the activation model that was successful for P3HT. This too was not successful for PEDOT, although this result is less surprising because PEDOT lacks side chains that possess the freedom to rotate as the appropriate thermal energy is provided.

We therefore explore a model developed by Rouse and Zimm.[32,40,43] Consider a polymer containing n chains per unit volume (cm^{-3}), in which each chain consists of Z submolecular units. The Rouse and Zimm theory expresses the frequency dependences $G'(\omega)$ and $G''(\omega)$ as[43]

$$G'(\omega) = nkT \sum_{p=1\ldots Z} \frac{\omega^2 \tau_p^{\,2}}{1 + \omega^2 \tau_p^{\,2}} \tag{4a}$$

$$G''(\omega) = nkT \sum_{p=1\ldots Z} \frac{\omega \tau_p}{1 + \omega^2 \tau_p^{\,2}} \tag{4b}$$

where the index p denotes a particular normal mode with its own characteristic relaxation time, τ_p. Equations 4a and 4b represent the real and imaginary parts, respectively, of the Fourier transform of the time-dependent modulus with multiple relaxation times, τ_p.

The relaxation time is dependent on the viscosity (η) of the medium in which the chains are present. This relationship is described by[32]

$$\tau_p = \frac{6\eta}{n\pi^2 kTp^2} \tag{5}$$

Equation 5 may be understood qualitatively as representing the diffusion time required for a single rotation of a globule of diameter a around itself in a medium where its diffusion coefficient (D) is given by a^2/τ_p. On the basis of dimensional analysis, one can use the Stokes−Einstein relationship, $D = kT/6\pi\eta a$, with $n = a^{-3}$ to arrive at eq 5, with only the coefficient (involving π and p) undefined. In our experiments, we determine only the lowest frequency relaxation; thus, we restrict our analysis to the case of $p = 1$ only in eqs 4a and 4b.

Inspection of the G' data in Figure 5 shows a strong frequency dependence, though somewhat weaker than ω^2, between 10 and 30 MHz. This suggests (see eq 4) that $(\omega\tau_p)^2 \leq 1$ at 10 MHz and $\omega\tau_p \approx 1$ at 30 MHz. Thus, in interpreting the temperature dependence at the fundamental ($f = 10$ MHz) resonance (see Figure 4), we can neglect $(\omega\tau_1)^2$ compared to unity in the denominator of eq 4 so that

$$G' \approx nkT(\omega\tau_1)^2 \tag{6}$$

The validity of this approximation can be tested by making a numerical estimate of τ at 10 MHz, as follows. We first need to assume a value for the length of the chain segment that is involved in the relaxation process. A minimum physically realistic value is 10 monomer units, each of which has a "molar" mass of 140; the weight of this relaxing chain, M, is thus 1400 g mol^{-1}. Approximating the polymer density, ρ, as 1 g cm^{-3} and the density of chains, $n = N_A\rho/M$ (N_A is Avogadro's number), we calculate a value of 4.3×10^{20} cm^{-3}. The second stage is to estimate the viscosity, η, which is given by G''/ω, where $G'' = 1.5 \times 10^7$ dyn cm^{-2} (from Figure 4b) and $\omega = 2\pi \times 10^7$ Hz (at the resonator fundamental frequency). Inserting these values into eq 5, we obtain $\tau = 8 \times 10^{-9}$ s. Continuing, by inserting this value into eq 6, we obtain $G' = 4.5 \times 10^6$ dyn cm^{-2}, in remarkably good agreement with experiment, considering the approximations made.

The temperature dependence of the relaxation time as defined by eq 5 is primarily through the temperature dependence of the viscosity of the medium. This dependence can be described by a form of the Doolittle equation, which is based on the concept of free volume:[43,44]

$$\ln \eta = \ln A + B\frac{\upsilon - \upsilon_f}{\upsilon_f} = \ln A + B\frac{1}{f_g + \alpha(T - T_g)} \tag{7}$$

where A is a constant, B is another constant whose value is approximately unity, υ is the volume of the polymer, and υ_f is the free volume per unit mass. The ratio $f_g = \upsilon_{fg}/\upsilon_g$ is the fraction of free volume at the glass-transition temperature, T_g, and α is the coefficient of thermal expansion. According to Ferry,[43] T_g is the "temperature below which the free volume no longer collapses", no matter how slow the cooling is carried out.

By inserting eqs 5 and 7 into eq 6, one can obtain the variation of G' as a function of frequency and temperature:

$$\ln G'(\omega,T) = \frac{2}{f_g + \alpha(T - T_g(E))} + 2\ln\omega + \text{const} \tag{8}$$

Although we do not explore it, an analogous equation can be developed for G''. The only difference is the absence of the factor of 2 on the right-hand side (compare the squared and linear appearances of the $\omega\tau$ parameters in eqs 4a and 4b, respectively).

(43) Ferry, J. D. *Viscoelastic properties of polymers*; 1961, Chapters 10 and 11.

(44) Efimov, I.; Winkels, S.; Schultze, J. W. *J. Electroanal. Chem.* **2001**, *499*, 169−175.

The presentational form of Figure 2 made clear that the three control parameters at our disposal, and through which we intended to manipulate viscoelastic properties, were ω, T, and solvent content (via applied potential, E). The first two of these appear explicitly in eq 8. The solvent content cannot be controlled in a direct manner but is a function of applied potential through the variation with the potential of polymer charge state; the variation of solvent population is not linear, in general, [45] but nonetheless is widely acknowledged to be significant. We recognize this in eq 8 by indicating that the glass-transition temperature of the film is a function of applied potential, $T_g(E)$. The value of $T_g(E)$ for the film will depend on the glass-transition temperatures of the pure polymer and solvent components, T_g^P and T_g^S, respectively. T_g^S is simply the freezing point of the solvent, if we take the view that the film is permselective. (Small amounts of salt do not change the concept and only change the numerical outcome slightly.) Using X_P and $X_S(E)$, respectively, to represent the mole fractions of the polymer and solvent components within the film (subject to the constraint $X_p + X_S(E) = 1$), we can write

$$T_g(E) = X_P T_g^P + X_S(E) T_g^S(E) \qquad (9)$$

Equations 8 and 9, together with thermodynamically defined values of $X_S(E)$ and $T_g^S(E)$, describe the behavior of $\mathbf{G}(\omega,T,E)$. For PEDOT, the dependence of both shear modulus components on E was found to be negligible, the dependence on T was quite small, and the dependence on ω was very dramatic. For the purpose of illustration, we will focus on the interpretation of the storage component, G'; the same outcomes result from analysis of G'', despite the potential difficulties of ensuring separation of this component from solution viscosity effects.

We apply eq 8 at a fixed potential. By normalizing the data with respect to G' at a reference temperature (chosen for convenience to be 20 °C), we eliminate the constant term so that

$$\ln\left(\frac{G'(T)}{G'(T_0)}\right) = \frac{2}{f_g + \alpha(T - T_g(E))} - \frac{2}{f_g + \alpha(T_0 - T_g(E))} \qquad (10)$$

G' data at $E = 0.3$ V and the fit to eq 10 are shown in Figure 6. Nonlinear fitting yields $\alpha = 1.3 \times 10^{-4}$ K^{-1} and $f_g = 0.16$. The value for the thermal expansion coefficient is typical of many polymers.[43] The low value provides an explanation for the relatively small effect of temperature on shear modulus components. The fraction of free volume at T_g is somewhat larger (by a factor of ca. 5−7) than that for many bulk polymers.[32,40,43] However, we note that this can vary appreciably with monomer structure (notably side-chain effects) such that it may be a consequence of the specific electropolymerization and deposition process conditions used (PEDOT films are known to be porous[12]) and, more generally, that we cannot presume thin films behave exactly the same as bulk materials. The small value of α makes estimation of T_g difficult, but a rough estimate is about 10 °C; we therefore omitted from Figure 6 the data at 0 °C for which $T < T_g$ so that eq 10 is inappropriate.

The relative values of f_g and α mean that the first of the two terms in each of the denominators of eq 10 is much larger than the second. We can then expand the expression as a binomial series and retain only the first term. After a little algebra, the simple linear result is

$$\ln[G'(T)/G'(T_0)] = -(2\alpha/f_g^2)(T - T_0) \qquad (11)$$

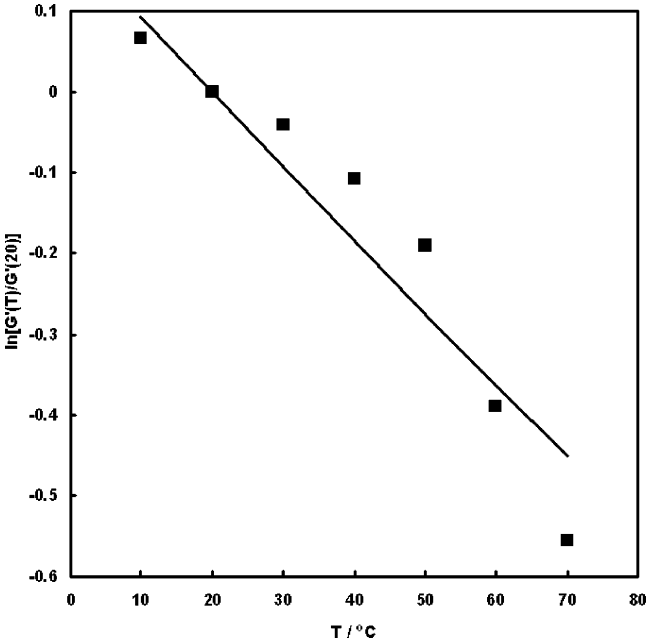

Figure 6. Data for G' (Figure 5) at $E = 0.3$ V plotted according to eq 10. The solid line shows fitting to the linear approximation of eq 11 (which is not significantly different from the nonlinear fit to eq 10; see text).

A linear fit to the data (see Figure 6) yields $\alpha/f_g^2 = 0.0100$, which is not too different from the value of 0.0083 obtained from nonlinear fit values given the approximations made and the experimental uncertainties. Although the difference between the linear and nonlinear variants of the equation is not significant, the model is clearly not a perfect representation of the data. We speculate that this is a consequence of the simplification we have made by restricting our application of the general Rouse model to a single relaxation time, although the real material may have two or more relaxation times; mathematically, this corresponds to our restriction to the leading, $p = 1$, term in eq 4 . To explore this hypothesis would require the additional application of a direct structural probe, which is beyond the scope of the present study. Nonetheless, when one considers the expanded scale for the ordinate of the plot in Figure 6, it is clear that the simplified version of the Rouse model does a reasonable job of describing a complex system at a conceptually simple level through the use of a small number of parameters taking physically sensible values.

Conclusions

In the context of the thickness of shear mode acoustic wave devices, the combination of systematically varying potential (E), temperature (T), and frequency (ω) provides a powerful means of exploring the viscoelastic properties of electroactive films. We are able to quantify these properties in terms of film shear moduli ($\mathbf{G} = G' + jG''$). The effect of E on $\mathbf{G}$ is indirect via redox driven changes in the film solvent content, that of T is associated with variation in the dynamics of activated process-(es), and that of ω (via resonator harmonics) is a change in the

(45) Bruckenstein, S.; Hillman, A. R. *J. Phys. Chem. B* **1998**, *102*, 10826−10835.

observational time scale on which these dynamics are viewed. Quite generally, different underlying (sub)molecular processes can be expected to be associated with different $\mathbf{G}(E,T,\omega)$ signatures.

In the specific case of poly(3,4-ethylenedioxythiophene) (PEDOT) films exposed to acetonitrile solutions and maintained under potential control, we have used this strategy to characterize the dynamics of undoped and p-doped films in unprecedented detail; n-doped films have been explored in a rather less detailed manner, as a consequence of limited film stability over the extended periods of time required to explore $\mathbf{G}(E,T,\omega)$ space. Under all conditions employed, PEDOT films have shear moduli that place them in the viscoelastic regime. Surprisingly, the variation of **G** with E is barely measurable, and the variation with T is very modest. In contrast, the effect of frequency (varied over the range 10−110 MHz) is dramatic.

The values of **G** and the changes with E, T, and ω are quite different from those recently observed for another member of the polythiophene family, poly(3-hexylthiophene), for which activated motion of the alkyl side chains was concluded to be the primary process controlling viscoelastic properties. The closed-ring ether substituents in PEDOT clearly do not offer this opportunity for intramolecular motion. Instead, we find that a model based on free volume is able to rationalize the functional dependence of **G** on the control parameters.

Acknowledgment. We thank the EPSRC (GR/N00968) and the University of Leicester for financial support.

JA054259Z